Quantum entanglement in the non-Hermitian frustrated triangular lattice

Yaman Evkaya[1, *] and Ekrem Aydiner[2, 3, †]

[1] *Ludwig-Maximilians-Universität München, Theresienstr. 37, München, Germany*
[2] *Theoretical and Computational Physics Research Laboratory, İstanbul University, 34134 İstanbul, Türkiye*
[3] *Department of Physics, Faculty of Science, İstanbul University, 34134 İstanbul, Türkiye*

(Dated: February, 2024)

In this work, we considered non-Hermitian XY and XX frustrated triangular quasi-one-dimensional isotropic dimerized quantum spin chains with the transverse complex field. We transformed the system to the spinless fermionic system by using the fermionization transform of Jordan-Wigner and then used the Fourier transform and the Bogoliubov transformation to diagonalize the Hamiltonian. We analytically obtained energy eigenvalues of transformed Hamiltonians. Thus, we have shown that the non-Hermitian frustrated dimerized triangle Heisenberg spin system can be solved exactly with this method. Furthermore, we have shown that, for quantum entanglement, both systems go to the classical limit for high temperature and low magnetic field. Later on, we computed the entanglement entropy and the ground state entropy by using energy eigenvalues for the XY and XX Hamiltonians.

Keywords: Frustration, spin glass, non-Hermitian system, quantum entanglement.

I. INTRODUCTION

In recent years non-Hermitian physics [1] has attracted wide research interests. A wide variety of classical and quantum systems described by non-Hermitian matrices or operators together with their physical origins of non-Hermiticity such as photonic systems [2, 3], mechanics [4], electrical circuits [5], open systems [6, 7], optic systems [8, 9], electron-electron interaction [10, 11] and *etc.* The reader can find numerous articles and very important review articles on non-Hermitian physics in the literature (please see Refs. [12–16] and references in there).

Motivated by the Yang-Lee model, von Gehlen first analyzed the Ising quantum spin chain in the presence of a magnetic field in the z-direction as well as a longitudinal imaginary field to carry out critical and off-critical conformal properties of these systems [17]. In a similar study, Castro-Alvaredo and Fring discussed the magnetic properties of the non-Hermitian Ising quantum spin chain [18]. Alcaraz *et al* studied surface exponents of integrable XXZ spin chains with imaginary boundary magnetic fields [19]. Additionally, Korff studied XX spin-chain with non-Hermitian diagonal boundary conditions and showed that the system behaves as quasi-Hermitian for special values of boundary parameters [20]. Similarly, the non-Hermitian version of the quantum spin chain has also been studied in previous works [21–26]. For example, Zhang and Song studied the non-Hermitian version of the one-dimensional anisotropic XY model with intrinsic rotation-time reversal symmetry to discuss quantum phase transition in these systems [21]. They also analyzed the geometric phase and phase diagram for the non-Hermitian quantum XY model [22]. Li *et al* explored the quantum phase transition in non-Hermitian $\mathcal{PT}$-symmetric Ising model, which is driven by a staggered complex transverse field [23]. In a similar study, Li and Song studied the finite-temperature quantum criticality in a non-Hermitian $\mathcal{PT}$-symmetric Ising model [24]. Additionally, Li *et al* analyzed chern number in the one-dimensional non-Hermitian Ising model with spatially modulated real and complex fields [25]. Bi *et al* carried out the phase diagram and band structure of the non-Hermitian ring frustrated XY ring spin model [26].

Recently, the quantum entanglement in non-Hermitian systems has also become an interesting field. One can see that some pioneering work has been done on entanglement characteristics of non-Hermitian fermionic systems, such as the non-Hermitian topology and the quantum quenching in non-Hermitian Hamiltonians. For instance; Herviou *et al* discussed the entanglement spectrum and symmetries in non-Hermitian fermionic non-interacting models [27]. Chang *et al* analyzed the entanglement spectrum and the entropy of free-fermion systems without the Hermiticity by use of correlation matrix and overlap matrix in biorthogonal basis [28]. Bácsi and Dóra investigated a quantum quench from a critical to an exceptional point [29]. However, there are few studies on entanglement properties in non-Hermitian spin systems. Recently, Turkeshi and Schiró investigated entanglement and correlation spreading in non-Hermitian anisotropic XY model spin chains with a complex transverse field [30]. Li *et al* carried out the ground-state and thermal entanglements in a non-Hermitian XY system with real and imaginary magnetic fields [31].

* yevkaya@hotmail.com
https://orcid.org/0000-0003-0020-150X
† ekrem.aydiner@istanbul.edu.tr
https://orcid.org/0000-0002-0385-9916

In this paper, we will consider non-Hermitian XY and XX frustrated triangular quasi-one-dimensional isotropic and anisotropic dimerized quantum spin chains with the transverse complex field to discuss the entanglement in each system via using the Jordan-Wigner transformation to fermionize systems, Fourier and Bogoliubov transformations to diagonalize the Hamiltonian of the given system and finally computing entanglement entropy properties for each system.

This paper is organized as follows. In Sec. II, we present the non-Hermitian model and Hamiltonians with its exact solutions. The schematic structures of systems are illustrated in Sec. III. We reformulated the Hamiltonian in terms of spinless fermionic particles using the Jordan-Wigner transformation then we diagonalized the Hamiltonian by using the Fourier and the Bogolibov transformations. In Section IV, we computed the entanglement entropy and ground state entropy of the model by using the energy eigenvalues of each system. Finally, we give a conclusion and discussion in the last section.

II. THE MODEL AND HAMILTONIAN

The concept of frustration for spin systems was first introduced in the context of spin glass systems by Toulouse [32]. The existence of such interactions was first observed experimentally by Mydosh [33]. Frustrated spin systems emerge by combining spins with ferromagnetic and anti-ferromagnetic interactions into a new lattice. The best way to describe frustration is to show it on a square or triangular spin-lattice. Square and triangular lattice cells are given in Fig.1(a) and (b), respectively. Let the interaction between spin 1 and spin 2 on the square plate and the interaction between spin 1 and spin 3 be given as anti-ferromagnetic. Therefore, in the square cell, coupling parameters are chosen as $J_{12} > 0$ and $J_{13} > 0$. Now let's assume that the spin 2 and 3 simultaneously force the spin 4 into the anti-ferromagnetic interaction. However, spin 4 will not be able to satisfy this condition at the same time. In such cases, if the system becomes stuck in one of these conditions below a critical temperature, the system will have a frozen disorder. Thus, the system becomes frustrated. As a result, let's assume that the system is trapped as in Fig.1(a). In this case it will be $J_{24} > 0$ and $J_{34} < 0$. In this schema, the energy between spins 3 and 4 will be degenerate. On the other hand, the same situation is valid for spin 3 in the triangle cell. In this example, let spin 1 and spin 2 have anti-ferromagnetic interactions. Let's assume that spin 1 and spin 2 try to have an anti-ferromagnetic interaction with spin 3 at the same time. Similarly, this condition will not be met at the same time. Below the critical temperature, the system will be frozen and disordered, and the energy of one of these bonds will degenerate and the system will be frustrated. In this example, we assume that the bond between spin 2 and 3 degenerates and has ferromagnetic interaction as $J_{23} < 0$.

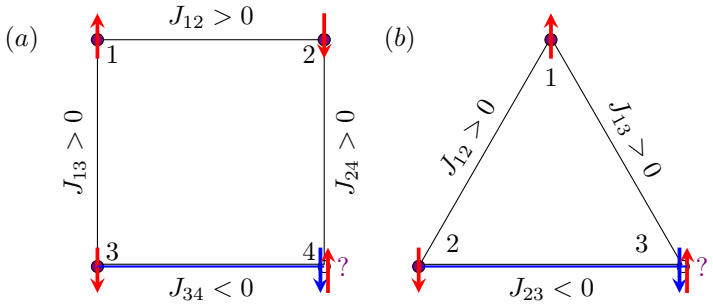


FIG. 1. Schematic representation of the quasi-one-dimensional frustrated antiferromagnetic spin chain.

In such geometries, if the product of signs of the interaction bond between spins is negative, the frustration condition is satisfied:

$$Sign = \prod_{(ij)\ \in\ loop} J_{ij} < 0 \tag{1}$$

as seen in Fig.1(a) and (b). Frustrated systems are very interesting systems in terms of physics. These systems cause the emergence of a magnetic phase known as spin-glass. Many materials exhibit spin glass properties and their magnetic properties have been studied in detail (see detailed review [34] and two nice books [35, 36]).

In this study, as we mentioned in the introduction part of the article, we will consider the fully frustrated quasi-one dimensional dimerized XY Heisenberg spin system whose schematic picture is given in Fig.2(a). Such spin systems

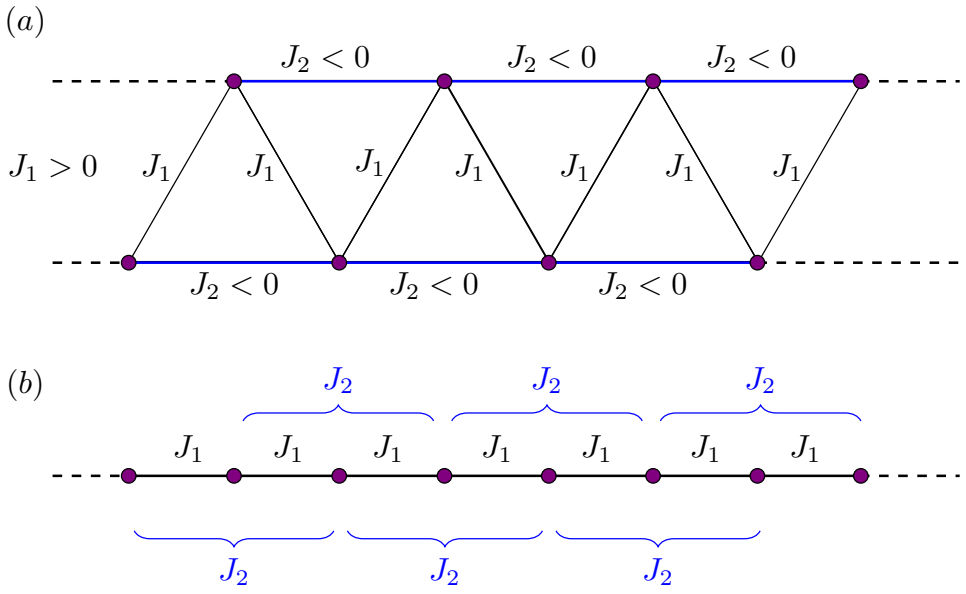


FIG. 2. The schematic representation of the quasi-one-dimensional fully frustrated dimerized spin chain.

are known as zig-zag ladder or dimerized spin systems. In this schematic picture, J_1 represents anti-ferromagnetic interactions and J_2 represents ferromagnetic interactions. Therefore, $J_1 > 0$ is chosen for the anti-ferromagnetic interaction and $J_2 < 0$ for the ferromagnetic interaction. Each triangle cell in Fig.2(a) satisfies the condition given in Eq.(1). As can be seen from the figure, the bonds shown in blue are degenerate. Therefore, the system ground state energy is degenerate. Here we will assume that an imaginary external magnetic field is applied to this system. As it is known, the imaginer magnetic field will transform the Hamiltonian of the spin system into a non-Hermitian $\mathcal{PT}$ symmetric form. This triangle dimerized system can be reduced to a one-dimensional discrete lattice, as can be seen in Fig.2(b). In this case, it becomes easier to write the Hamiltonian of the system.

The anisotropic-frustrated XY non-Hermitian Hamiltonian is given by

$$H = J_1 \sum_{<j>} \left\{\sigma_j^x \sigma_{j+1}^x + \sigma_j^y \sigma_{j+1}^y\right\} + J_2 \sum_{<<j>>} \left\{[\sigma_j^x \sigma_{j+2}^x + \sigma_j^y \sigma_{j+2}^y]\sigma_{j+1}^z\right\} + \gamma \sum_{<j>} \left\{\sigma_j^x \sigma_{j+1}^x - \sigma_j^y \sigma_{j+1}^y\right\} + i\delta \sum_{<j>} \left\{\sigma_j^x \sigma_{j+1}^y + \sigma_j^y \sigma_{j+1}^x\right\} \tag{2}$$

where we set $J_{1x} > 0$ and $J_{1y} > 0$ while $J_{2x} < 0$ and $J_{2y} < 0$ for the frustration condition. Eq.(**??**) has not only frustrated but also anisotropic-frustrated form. This equation reduces to the XX isotropic-frustrated form for $J_{1x} = J_{1y} > 0$ and $J_{2x} = J_{2y} < 0$:

$$H_{XX} = ... \tag{3}$$

where σ_j^α $(\alpha = x, y, z)$ components are Pauli spin-1/2 spin matrices, L is the size of the system. As we stated above, J_1 represents the antiferromagnetic interaction and J_2 represents the ferromagnetic interaction. In the third term δ represents the magnitude of the imaginary magnetic field. Here $< . >$ denotes nearest neighbor, and $<< . >>$ indicates next-nearest neighbour interactions.

III. REFORMULATION OF THE HAMILTONIAN

Before applying the Jordan-Wigner transformation we can write the Hamiltonian in Eq.(**??**) in a special form

$$H = \frac{J_1}{2}\sum_{<j>}\left\{\sigma_j^+\sigma_{j+1}^- + \sigma_j^-\sigma_{j+1}^+\right\} + \frac{J_2}{2}\sum_{<<j>>}\left\{[\sigma_j^+\sigma_{j+2}^- + \sigma_j^-\sigma_{j+2}^+]\sigma_{j+1}^z\right\} \tag{4}$$
$$+\frac{\gamma}{2}\sum_{<j>}\left\{\sigma_j^+\sigma_{j+1}^+ + \sigma_j^-\sigma_{j+1}^-\right\} + \frac{\delta}{2}\sum_{<j>}\left\{\sigma_j^+\sigma_{j+1}^+ - \sigma_j^-\sigma_{j+1}^-\right\}$$

where Pauli spin operators are neither bosonic nor fermionic. To obtain the entanglement entropy we will reformulate the Hamiltonian in Eq.(**??**) in this section. Therefore, by using the Jordan-Wigner [37] transformation, we will represent Pauli spin matrices in terms of fermionic operators. Jordan-Wigner transformations of the Pauli spin can be given as

$$\sigma_j^+ = c_j^\dagger \exp\left[-i\pi\sum_{l=1}^{j-1}c_l^\dagger c_l\right] \tag{5}$$

$$\sigma_j^- = \exp\left[-i\pi\sum_{l=1}^{j-1}c_l^\dagger c_l\right]c_j \tag{6}$$

$$\sigma_j^z = 2c_j^\dagger c_j - 1 \tag{7}$$

where $c_j^\dagger$ ve c_j are fermionic creation and annihilation operators. These operators satisfy standard anti-commutation relations $\{c_i, c_j\} = 0$ and $\{c_i, c_j^\dagger\} = 1$. The exponential terms in Eqs. (5) and (6) can be written as

$$Q_j = \exp\left[i\pi\sum_{l=1}^{j-1}c_l^\dagger c_l\right] = \prod_{l=1}^{j-1}(1 - 2c_l^\dagger c_l) \tag{8}$$

which satisfy $Q_j^2 = 1$. In this case, the Hamiltonian in Eq.(**??**) becomes

$$H = \frac{J_1}{2}\sum_{<j>}\left\{c_j^\dagger c_{j+1} + c_j c_{j+1}^\dagger\right\} + \frac{J_2}{2}\sum_{<<j>>}\left\{c_j^\dagger c_{j+2} + c_j c_{j+2}^\dagger\right\} \tag{9}$$
$$+\frac{\gamma}{2}\sum_{<j>}\left\{c_j^\dagger c_{j+1}^\dagger + c_j c_{j+1}\right\} + \frac{\delta}{2}\sum_{<j>}\left\{c_j^\dagger c_{j+1}^\dagger - c_j c_{j+1}\right\}$$
$$+(-1)^{\hat{N}}[\frac{J_1}{2}\sum_{<j>}\left\{c_N^\dagger c_{N+1} + c_N c_{N+1}^\dagger\right\} + \frac{J_2}{2}\sum_{<<j>>}\left\{c_N^\dagger c_{N+2} + c_j c_{N+2}^\dagger\right\}$$
$$+\frac{\gamma}{2}\sum_{<j>}\left\{c_N^\dagger c_{N+1}^\dagger + c_N c_{N+1}\right\} + \frac{\delta}{2}\sum_{<j>}\left\{c_N^\dagger c_{N+1}^\dagger - c_N c_{j+1}\right\}]$$

the last term represents the contribution of the boundary condition. $\hat{N}$ is called the parity operator. Eigenvalues of $\hat{N}$ are integer, and eigenvalues of the operator $(-1)^{\hat{N}}$ can only take on two distinct values, $+1$ and -1. After employing boundary conditions into Eq.(**??**) and combining some related terms, we obtain

$$H = \frac{J_1}{2}\sum_{<j>}\left\{c_j^\dagger c_{j+1} + c_j c_{j+1}^\dagger\right\} + \frac{J_2}{2}\sum_{<<j>>}\left\{c_j^\dagger c_{j+2} + c_j c_{j+2}^\dagger\right\} \tag{10}$$
$$+\sum_{<j>}\left\{\frac{\gamma+\delta}{2}(c_j^\dagger c_{j+1}^\dagger) + \frac{\gamma-\delta}{2}(c_j c_{j+1})\right\}$$

Now, we are ready to diagonalize the Hamiltonian in Eq.(**??**). The first step is to go to the Fourier space by defining a new set of operators c_k according to

$$c_k = \frac{1}{\sqrt{L}}\sum_j c_j e^{ikj} \tag{11}$$

In the case of H_+ we should have $c_{L+1} = c_1$ (periodic bc), so we must have $e^{ikL} = -1$, however, we have have $e^{ikL} = 1$ for $c_{L+1} = c_1$ (periodic bc.). We can write

$$k = \frac{\pm(2l+1)\pi}{L}, \qquad l = 0, 1, ..., \frac{L}{2} - 1 \tag{12}$$

for the anti-periodic bc. and

$$k = \frac{\pm 2l\pi}{L}, \qquad l = 1, ..., \frac{L}{2} - 1 \tag{13}$$

for the periodic bc. These conditions satisfy usual Fourier orthogonality relations. Now we define $\frac{\gamma+\delta}{2} \equiv \alpha_1$ and $\frac{\gamma-\delta}{2} \equiv \alpha_2$ terms. After the Fourier transformation, we get Fourier dönüşümü;

$$\frac{1}{2}\sum_k \left\{ \left(J_1(e^{ik} + e^{-ik}) + J_2(e^{2ik} + e^{-2ik}) \right) c_k^\dagger c_k + (\alpha_1 e^{ik} c_k^\dagger c_{-k}^\dagger + \alpha_2 e^{-ik} c_k c_{-k}) \right\} \tag{14}$$

At this point, one can see that the Hamiltonian is not yet diagonal, which involves pairs $(k, -k)$ of fermions. Therefore, to diagonalize this Hamiltonian we will use the Bogoluibov transformation [38–42]. Before doing so, we can do some interventions over this Hamiltonian (**??**) and show the symmetry more clearly. To do this, we expand the origin of the Brillouin zone and rewrite the Hamiltonian (**??**) via combining the k and $-k$ terms and summing over one half of the Brillouin zone, $0 \leq k \leq \pi$. As a result, we can write 1. Brillouin Zone genişletmesi;

$$\frac{1}{2}\sum_k \left\{ \left(J_1(e^{ik} + e^{-ik}) + J_2(e^{2ik} + e^{-2ik}) \right) \left(c_k^\dagger c_k + c_{-k}^\dagger c_{-k} \right) + (\alpha_1(e^{ik} - e^{-ik}) c_k^\dagger c_{-k}^\dagger + \alpha_2(e^{ik} - e^{-ik}) c_k c_{-k}) \right\} \tag{15}$$

If we insert trigonometric functions

$$\sum_k \left\{ (J_1 \cos k + J_2 \cos 2k) \left(c_k^\dagger c_k + c_{-k}^\dagger c_{-k} \right) + i \sin k \left(\alpha_1 c_k^\dagger c_{-k}^\dagger + \alpha_2 c_k c_{-k} \right) \right\} \tag{16}$$

This Hamiltonian can be written in a more compact form as

$$\mathcal{H} = ... \tag{17}$$

Now, to diagonalize the matrix in Eq.(17), we can apply the Bogoluibov transformation

$$\eta_k = u_k c_k^\dagger + i\sqrt{\frac{\alpha_2}{\alpha_1}} \nu_k c_k \tag{18}$$

$$\eta_k^\dagger = u_k c_{-k} - i\sqrt{\frac{\alpha_1}{\alpha_2}} \nu_k c_k^\dagger \tag{19}$$

where $u_k = \cos(\theta_k)$ and $\nu_k = \sin(\theta_k)$ which ensures the $|u_k|^2 + |\nu_k|^2 = 1$ relation.

$$\theta_k = ... \tag{20}$$

If we rewrite the u_k and ν_k

$$u_k = \frac{|\sin k| \sqrt{\alpha_1 \alpha_2}}{\sqrt{2\varepsilon_k(\varepsilon_k + J_1 \cos k + J_2 \cos 2k)}} \tag{21}$$

$$\nu_k = sgn(\sin k) \sqrt{\frac{\varepsilon_k + J_1 \cos k + J_2 \cos 2k}{2\varepsilon_k}} \tag{22}$$

Here we apply some interventions to diagonalize the Hamiltonian

$$\mathcal{H}_\mathcal{K} = ... \tag{23}$$

This result can be written in a more formal form as

$$\mathcal{H}_\mathcal{K} = U_k^\dagger \begin{pmatrix} \varepsilon_{(k)} & 0 \\ 0 & -\varepsilon_{(k)} \end{pmatrix} U_k \tag{24}$$

where

$$U_k = \begin{pmatrix} U_k & \nu_k \\ \nu_k^\dagger & u_k^\dagger \end{pmatrix} = \begin{pmatrix} \cos\theta_k & i\sin\theta_k \\ -i\sin\theta_k & \cos\theta_k \end{pmatrix} \tag{25}$$

$$\mathcal{H}_{\mathcal{XY}} = \sum_{k=0}^{\pi} \psi^\dagger \mathcal{H}_k \psi = \sum_{k=0}^{\pi} \psi^\dagger U_k^\dagger \begin{pmatrix} \varepsilon_{(k)} & 0 \\ 0 & -\varepsilon_{(k)} \end{pmatrix} U_k \psi \tag{26}$$

$$U_k \psi_k = \begin{pmatrix} \eta_k \\ \eta_{-k}^\dagger \end{pmatrix} \tag{27}$$

Finally, the Hamiltonian (17) can be diagonalized and which will then become

$$\mathcal{H}_{\mathcal{XY}} = \sum_{k=-\pi}^{\pi} \varepsilon(k)(\eta_k^\dagger \eta_k + \frac{1}{2}) \tag{28}$$

where

$$\varepsilon_k = \sqrt{(J_1 \cos k + J_2 \cos 2k)^2 + (\alpha_1 \alpha_2 \sin^2 k)} \tag{29}$$

is energy eigenvalues of the frustrated XY Hamiltonian in Eq.(**??**). For the $J_{1x} = J_{1y} = J_1 > 0$ and $J_{2x} = J_{2y} = J_2 < 0$, this result reduces to

$$\varepsilon_{(k)} = ... \tag{30}$$

refers to energy eigenvalues of the frustrated XX Hamiltonian in Eq.(3).

Finally, in this section, we reformulated the Hamiltonian for frustrated dimerized systems given in Fig.2 and the corresponding Hamiltonian in Eq.(**??**). We constructed a diagonalized Hamiltonian for Eq.(**??**) and we obtained energy eigenvalues of the system. Now we can discuss the entanglement phenomena of each system in the next section.

IV. ENTANGLEMENT ENTROPIES AND NUMERICAL RESULTS

In this section, firstly, by using two different methods, we will compute the thermal entanglement entropy and the ground state entanglement entropy of the non-hermitian XY and XX frustrated dimerized spin systems given in Eqs. (**??**) and (3).

A. The Thermal Entanglement Entropy

Now, we are going to examine the entanglement entropy of non-Hermitian XX and XY systems for various external magnetic fields. Therefore, to discuss the entanglement entropy we need to compute the free energy of systems. The partition function for this system can be written as

$$Z\left(T,N\right) = \sum_{k=0} e^{-\beta \mathcal{H}} \tag{31}$$

or, using the Hamiltonian in Eq.(28), the partition function can be represented in terms of energy eigenvalues as

$$Z\left(T,N\right) = \sum_{k=0} e^{-\beta \sum_k \varepsilon_k (\eta_k^\dagger \eta_k - \frac{1}{2})} \tag{32}$$

where ε_k denotes energy eigenvalues given in Eq.(**??**). This function can be reorganized as

$$Z\left(T,N\right) = \sum_k \prod_k e^{-\beta \varepsilon_k (\eta_k^\dagger \eta_k - \frac{1}{2})} \simeq \prod_k 2\cosh(\frac{\beta \varepsilon_k}{2}). \tag{33}$$

By using the partition function, the free energy[43] per site is given by

$$f\left(T\right) = -\frac{1}{\beta} \lim_{N\to\infty} \frac{\log Z\left(T,N\right)}{N} = -\frac{1}{\beta} \lim_{N\to\infty} \frac{\log \prod_k 2\cosh(\frac{\beta\varepsilon_k}{2})}{N} \tag{34}$$

or

$$f\left(T\right)=-\frac{1}{\beta}\lim_{N\to\infty}\frac{1}{N}\sum_{k}\log(2\cosh(\frac{\beta\varepsilon_k}{2}))=-\frac{1}{2\pi\beta}\int_{-\pi}^{\pi}dk\log(2\cosh(\frac{\beta\varepsilon_k}{2})). \tag{35}$$

Here we can use the Fermi-Dirac distribution to express the following quantities.

$$n_k=\frac{1}{e^{\beta\varepsilon_k}+1} \tag{36}$$

Thus, the free energy per site becomes;

$$\begin{aligned} f\left(T\right)&=-\frac{T}{2\pi}\int_{-\pi}^{\pi}dk\log(2\cosh(\frac{\beta\varepsilon_k}{2}))=-\frac{T}{2\pi}\int_{-\pi}^{\pi}dk\log(e^{\frac{\beta\varepsilon_k}{2}}+e^{\frac{-\beta\varepsilon_k}{2}})\\ &=-\frac{T}{2\pi}\int_{-\pi}^{\pi}dk\log(e^{\frac{\beta\varepsilon_k}{2}}(e^{\beta\varepsilon_k}+1))=\frac{1}{2\pi}\int_{-\pi}^{\pi}dk(\frac{\varepsilon_k}{2}+T\log n_k) \end{aligned} \tag{37}$$

Now, we can extract entanglement phenomena in terms of the free energy. Before doing so let us take the derivative of the Fermi-Dirac distribution

$$\frac{\partial n_k}{\partial T}=n_k(1-n_k)\frac{1}{T^2}\varepsilon_k. \tag{38}$$

After a little bit of algebra, the thermal entropy can be given as;

$$S(T)=-\left(\frac{\partial f}{\partial T}\right)=-\frac{1}{2\pi}\int_{-\pi}^{\pi}dk(\log n_k+\frac{\varepsilon_k}{T}(1-n_k)). \tag{39}$$

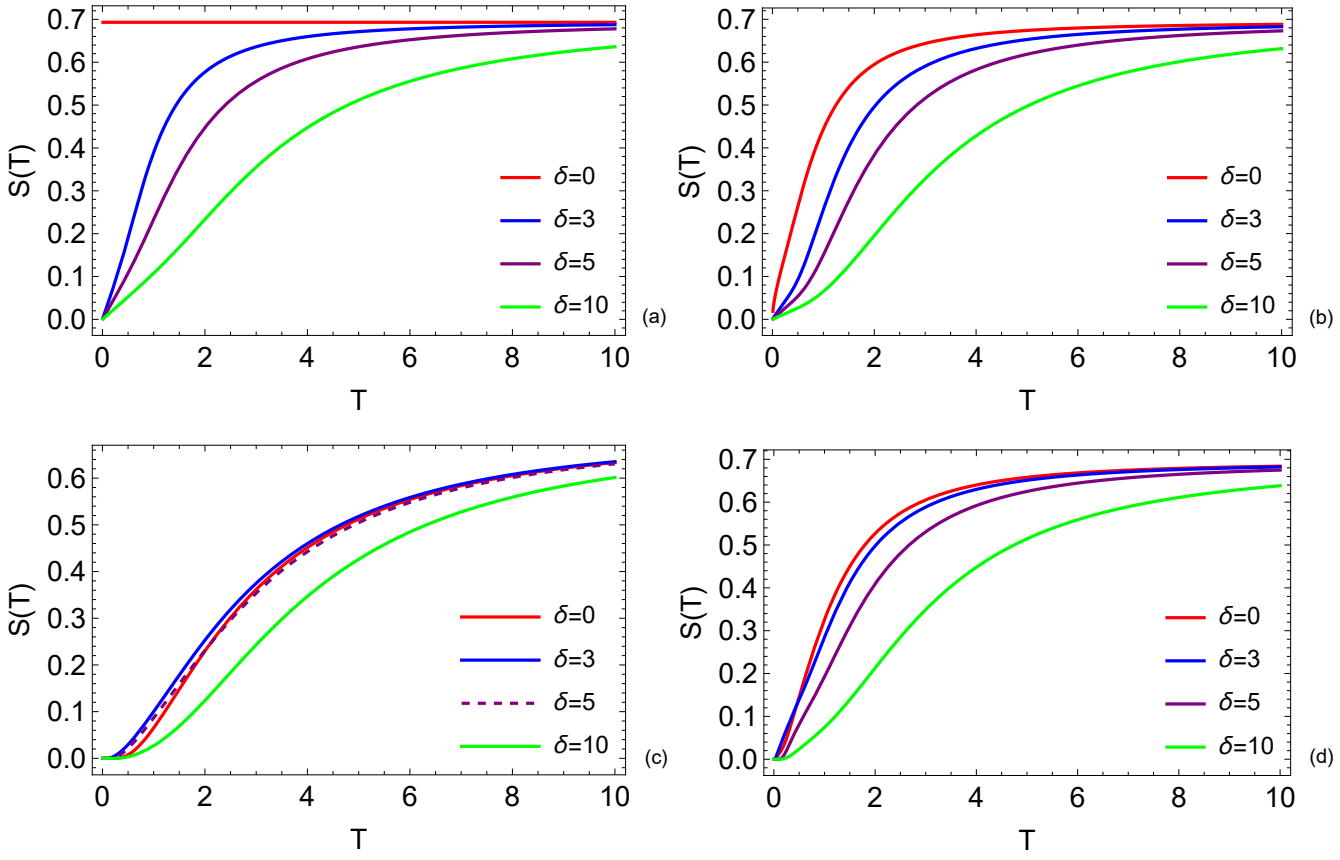


FIG. 3. The thermal entropy versus the temperature for various δ and coupling constant parameters.

Now, we will discuss the temperature dependence of the thermal entanglement entropy behavior for the various coupling parameters i.e., frustrated XX and XY systems in Eqs. (**??**) and (3). In Fig.3, thermal entropy numerical solutions are given.

In Fig.3(a) spin coupling parameters $J_{1x}=0$, $J_{1y}=0$ and $J_{2x}=0$, $J_{2y}=0$ were chosen. In this case, only the contribution comes from the term in which the external magnetic field is located. Fig.3(a) while selected interaction parameters are fixed, numerical solutions are shown according to different δ parameters. As can be seen, when $\delta=0$, the thermal entropy value is around 0.7. This solution is independent of the temperature and corresponds to the $\ln 2$ solution. On the other hand, for small values of δ ($\delta=3$ and $\delta=5$), the entropy increases faster in small temperature ranges and saturates at 0.7, while for large values of δ ($\delta=10$) increases more slowly and becomes saturated.

In Fig.3(b) spin coupling parameters $J_{1x}=1$, $J_{1y}=1$ and $J_{2x}=-1$, $J_{2y}=-1$ were chosen. In this case, the system behaves like a frustrated XX Hamiltonian. Fig.3(b) While selected interaction parameters are fixed, numerical solutions for different δ parameters are shown. As can be seen from the figure, for small values of δ ($\delta=0$, $\delta=3$ and $\delta=5$), the entropy increases faster in small temperature ranges and saturates at 0.7, while δ For large values of delta ($\delta=10$), it increases more slowly and saturates.

In Fig.3(c) spin coupling parameters $J_{1x}=3$, $J_{1y}=5$ and $J_{2x}=-2$, $J_{2y}=-4$ were chosen. In this case, the system behaves like a frustrated XY Hamiltonian. Fig.3(c) While selected interaction parameters are fixed, numerical solutions are shown for different δ parameters. As can be seen from the figure, the entropy increases slowly for small values of δ ($\delta=0$, $\delta=3$ and $\delta=5$) in small temperature ranges and reaches 0.7 for high values of T. While it saturates, for larger values of δ ($\delta=10$) it saturates more slowly. It can be seen from Fig.3(c) that for this parameter selection, the entropy of $\delta=0$, $\delta=3$ and $\delta=5$ takes similar values.

In Fig.3(d) spin coupling parameters $J_{1x}=0.5$, $J_{1y}=1.5$ and $J_{2x}=-2$, $J_{2y}=-1$ were chosen. In this case, the system again behaves like the frustrated XY Hamiltonian. Fig3(d) While the selected interaction parameters are fixed, numerical solutions are shown for different δ parameters. As can be seen from the figure, the entropy increases slowly for small values of δ ($\delta=0$, $\delta=3$ and $\delta=5$) in small temperature ranges and reaches 0.7 for high values of T. While it saturates, for larger values of δ ($\delta=10$) it saturates more slowly. Again, it can be seen from Fig.3(d) that entropy values for $\delta=0$, $\delta=3$, and $\delta=5$ are close to each other.

B. The Ground State Quantum Entanglement

Now, we will investigate the ground state quantum entanglement using the generalized Gibbs ensemble approximation [44–48]. This method allows us to compute the ground state quantum entanglement. According to the method, the system is quenched to the ground state, later, the entanglement entropy is computed based on a two-point correlation function.

The ground-state reduced density matrix in Refs. [44–48] is described as

$$\rho=\frac{1}{Z}\exp(-\sum_k \varepsilon_k\xi_k) \tag{40}$$

where ε_k represents the given eigenvalue of our fermionic lattice in Eq.(**??**) and we can define ξ_k as $\xi_k=\eta_k^\dagger\eta_k$ which holds the condition of;

$$\mathrm{Tr}[\xi_k\rho]=\langle\xi_k\rangle=-\frac{\partial}{\partial\varepsilon_k}\ln Z \tag{41}$$

We can call the partition function Z in the form of;

$$Z=\mathrm{Tr}[\exp(-\sum_k\varepsilon_k\xi_k)]=\prod_k\sum_{n_k=0}^{\infty}\exp(-\varepsilon_k\xi_k)=\prod_k(1+\exp(-\varepsilon_k)) \tag{42}$$

Thus, if we rewrite our ξ_k;

$$\langle\xi_k\rangle=\frac{\partial}{\partial\varepsilon_k}\sum_k\ln\left(1+e^{-\varepsilon_k}\right)=\frac{1}{e^{\varepsilon_k}+1} \tag{43}$$

With the help of this information, we can produce the entanglement entropy by using the von Neumann definition [49–51].

$$S_{VN}=-\mathrm{Tr}(\rho\ln\rho) \tag{44}$$

$$=-\mathrm{Tr}\left(\frac{1}{\mathcal{Z}}\exp[-\sum_k\varepsilon_k\xi_k]\ln(\frac{1}{\mathcal{Z}}\exp[-\sum_k\varepsilon_k\xi_k])\right) \tag{45}$$

$$=\sum_k\left[-\varepsilon_k\frac{\partial\ln Z}{\partial\varepsilon_k}+\ln\mathcal{Z}\right] \tag{46}$$

If we insert the definition of Z, we get the final form of the von Neumann entropy as;

$$S_{VN} = -\sum_{k=0}^{N-1}\left[\frac{\varepsilon_k}{1+e^{\varepsilon_k}} + \ln(1+e^{\varepsilon_k})\right] = -\sum_{k=0}^{N-1}\xi_k \ln \xi_k + (1-\xi_k)\ln(1-\xi_k). \tag{47}$$

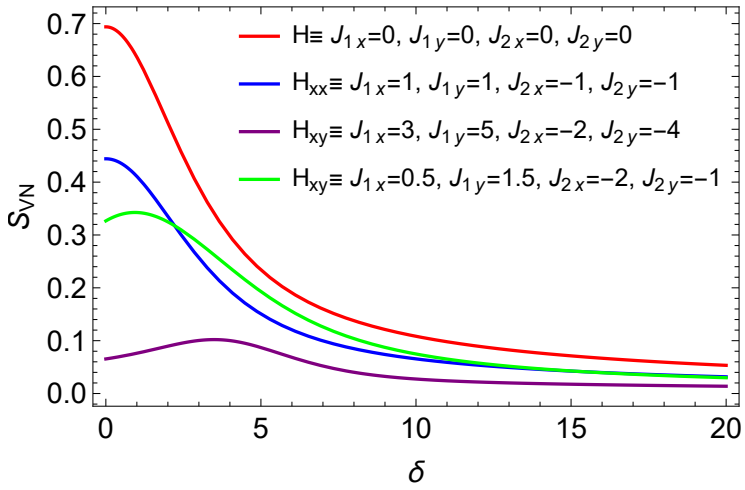


FIG. 4. The ground state von Neumann quantum entanglement entropy for various coupling constant values.

In this section, considering the von Neumann formalism, we examined the change of the entanglement entropy depending on the applied external field for non-Hermitian XY, and XX systems. Obtained numerical results are presented in detail in Fig.4. As seen from Fig.4, for example; firstly, we chose spin coupling parameters $J_{1x} = 0$, $J_{1y} = 0$ and $J_{2x} = 0$, $J_{2y} = 0$. The solution for these parameters is given by the red curve. When these parameters are chosen in this way, we obtain the behavior of only the term in which the magnetic field is applied. As can be seen, the curve decreases smoothly starting from 0.7 for $\delta = 0$. However, as δ increases, the von Neumann entanglement goes to its limit value. The limit value for each curve changes according to their chosen parameters (in all cases they are over close to zero). Secondly, we chose $J_{1x} = 1$, $J_{1y} = 1$ and $J_{2x} = -1$, $J_{2y} = -1$. For these coupling parameter values, our system turns into the XX spin Hamiltonian in Eq.(3). These parameter values ensure that the XX system is both isotropic and frustrated. The corresponding von Neumann entanglement is given by the blue curve. The maximum value of this value for $\delta = 0$ is around 4.5. Similarly, as δ increases, the entanglement value quickly goes to zero. Thirdly, we chose spin interaction parameters $J_{1x} = 3$, $J_{1y} = 5$ and $J_{2x} = -2$, $J_{2y} = -4$. This selection of the system leads to the Hamiltonian given in Eq.(**??**). These parameter values ensure that the XY system is both anisotropic and frustrated. This solution is given by the purple curve. As can be seen from the figure, for these values of the parameter, the von Neumann entanglement value at the beginning of the XY system is around 0.1. In other words, for this parameter value, the entanglement first increases steadily to very close to 0.1 until δ is approximately 0.35, and then slowly decreases vertically to its limit value. However, for the selection of different parameter values, for example, $J_{1x} = 0.5$, $J_{1y} = 1.5$ and $J_{2x} = -2$, $J_{2y} = -4$, the system still is an anisotropic frustrated XY system. However, as can be seen from the green curve for these values, the entanglement entropy value is above 0.3 for $\delta = 0$, and with the slight increase in the magnetic value, it first increases slightly and then decreases smoothly and goes to its limit value. This shows us that the choice of parameter values affects the entanglement in both systems, that is, in both XX and XY frustrated spin dimerized spin systems. However, in all cases, regardless of the choice of parameter values, the quantum entanglement entropy starts from a positive value for $\delta = 0$ and quantum entanglement very almost disappears as δ increases. This is an expected situation. While the external magnetic field is zero the two-spin Bell entanglement is maximum, the entanglement disappears with the increase of the magnetic field. We can say that a similar situation applies to the Hamiltonians we chose.

V. CONCLUSION

In this work, we considered a non-Hermitian XY and XX frustrated triangular quasi-one-dimensional isotropic dimerized quantum spin chain with the transverse complex field. We transformed this system into a spinless fermionic

system by using the Jordan-Wigner transformation. Additionally, We applied the Fourier and the Bogoliubov transformations to diagonalize the fermionic, frustrated non-Hermitian XY Hamiltonian. As a result, we obtained energy eigenvalues of the transformed Hamiltonian for non-Hermitian XY and XX Hamiltonians. Thus, we have shown that the non-Hermitian frustrated dimerized triangle Heisenberg spin system can be solved exactly with this method.

Furthermore, using two different methods, we computed the thermal entanglement entropy and the ground state quantum entanglement entropy for each non-Hermitian system. Firstly, we obtained the behavior of the entanglement entropy based on the free energy of the system. We see that two different methods produce related results at some points. For example; the entanglement entropy value for $\delta = 0$ is the same as the value of the thermal entropy for higher temperature values which satisfies the classical limit condition $\ln 2$. Secondly, we obtained the ground state quantum entanglement in terms of the von Neumann entropy based on stationary state conditions held by the Gibbs ensemble approximation [49–51] by using the long time limit which imposes the general behavior of the system is independent of thermal variables. In this way, we rescued our reduced density matrix from thermalization and were able to write it without the dependence on thermal variables. As a result, we have shown that the quantum entanglement for both thermodynamic and von Neumann formalism reaches the classical limit condition for high temperature and low magnetic field respectively for each non-Hermitian XY and XX Hamiltonians.

[1] C. M. Bender and S. Boettcher, Real spectra in non-hermitian hamiltonians having $\mathcal{PT}$ symmetry, Phys. Rev. Lett. **80**, 5243 (1998).
[2] A. Ruschhaupt, F. Delgado, and J. G. Muga, Physical realization of $\mathcal{PT}$-symmetric potential scattering in a planar slab waveguide, Journal of Physics A: Mathematical and General **38**, L171 (2005).
[3] R. El-Ganainy, K. G. Makris, D. N. Christodoulides, and Z. H. Musslimani, Theory of coupled optical $\mathcal{PT}$-symmetric structures, Opt. Lett. **32**, 2632 (2007).
[4] C. L. Kane and T. C. Lubensky, Topological boundary modes in isostatic lattices, Nature Physics **10**, 39–45 (2013).
[5] Y. N. Joglekar and S. J. Wolf, The elusive memristor: properties of basic electrical circuits, European Journal of Physics **30**, 661–675 (2009).
[6] H. J. Carmichael, Quantum trajectory theory for cascaded open systems, Phys. Rev. Lett. **70**, 2273 (1993).
[7] S. Malzard, C. Poli, and H. Schomerus, Topologically protected defect states in open photonic systems with non-hermitian charge-conjugation and parity-time symmetry, Phys. Rev. Lett. **115**, 200402 (2015).
[8] K. G. Makris, R. El-Ganainy, D. N. Christodoulides, and Z. H. Musslimani, Beam dynamics in $\mathcal{PT}$ symmetric optical lattices, Phys. Rev. Lett. **100**, 103904 (2008).
[9] S. Klaiman, U. Günther, and N. Moiseyev, Visualization of branch points in $\mathcal{PT}$-symmetric waveguides, Phys. Rev. Lett. **101**, 080402 (2008).
[10] H. Shen and L. Fu, Quantum oscillation from in-gap states and a non-hermitian landau level problem, Phys. Rev. Lett. **121**, 026403 (2018).
[11] M. Papaj, H. Isobe, and L. Fu, Nodal arc of disordered dirac fermions and non-hermitian band theory, Phys. Rev. B **99**, 201107 (2019).
[12] C. M. Bender, Introduction to $\mathcal{PT}$-symmetric quantum theory, Contemporary Physics **46**, 277 (2005), https://doi.org/10.1080/00107500072632.
[13] C. M. Bender, Making sense of non-hermitian hamiltonians, Reports on Progress in Physics **70**, 947 (2007).
[14] P. Dorey, C. Dunning, and R. Tateo, The ode/im correspondence, Journal of Physics A: Mathematical and Theoretical **40**, R205–R283 (2007).
[15] A. Mostafazadeh, Pseudo-hermitian representation of quantum mechanics, International Journal of Geometric Methods in Modern Physics **07**, 1191–1306 (2010).
[16] Y. Ashida, Z. Gong, and M. Ueda, Non-hermitian physics, Advances in Physics **69**, 249–435 (2020).
[17] G. von Gehlen, Critical and off-critical conformal analysis of the ising quantum chain in an imaginary field, Journal of Physics A: Mathematical and General **24**, 5371 (1991).
[18] O. A. Castro-Alvaredo and A. Fring, A spin chain model with non-hermitian interaction: the ising quantum spin chain in an imaginary field, Journal of Physics A: Mathematical and Theoretical **42**, 465211 (2009).
[19] F. C. Alcaraz, M. N. Barber, M. T. Batchelor, R. J. Baxter, and G. R. W. Quispel, Surface exponents of the quantum XXZ, ashkin-teller and potts models, Journal of Physics A: Mathematical and General **20**, 6397 (1987).
[20] C. Korff, Pt symmetry of the non-hermitian XX spin-chain: non-local bulk interaction from complex boundary fields, Journal of Physics A: Mathematical and Theoretical **41**, 295206 (2008).
[21] X. Z. Zhang and Z. Song, Non-hermitian anisotropic XY model with intrinsic rotation-time-reversal symmetry, Phys. Rev. A **87**, 012114 (2013).
[22] X. Z. Zhang and Z. Song, Geometric phase and phase diagram for a non-hermitian quantum XY model, Phys. Rev. A **88**, 042108 (2013).
[23] C. Li, G. Zhang, X. Z. Zhang, and Z. Song, Conventional quantum phase transition driven by a complex parameter in a non-hermitian $\mathcal{PT}-$symmetric ising model, Phys. Rev. A **90**, 012103 (2014).
[24] C. Li and Z. Song, Finite-temperature quantum criticality in a complex-parameter plane, Phys. Rev. A **92**, 062103 (2015).

[25] C. Li, G. Zhang, and Z. Song, Chern number in ising models with spatially modulated real and complex fields, Phys. Rev. A **94**, 052113 (2016).

[26] S. Bi, Y. He, and P. Li, Ring-frustrated non-hermitian XY model, Physics Letters A **395**, 127208 (2021).

[27] L. Herviou, N. Regnault, and J. H. Bardarson, Entanglement spectrum and symmetries in non-Hermitian fermionic non-interacting models, SciPost Phys. **7**, 069 (2019).

[28] P.-Y. Chang, J.-S. You, X. Wen, and S. Ryu, Entanglement spectrum and entropy in topological non-hermitian systems and nonunitary conformal field theory, Physical Review Research **2**, 033069 (2020).

[29] Á. Bácsi and B. Dóra, Dynamics of entanglement after exceptional quantum quench, Physical Review B **103**, 085137 (2021).

[30] X. Turkeshi and M. Schiró, Entanglement and correlation spreading in non-hermitian spin chains, Physical Review B **107**, 10.1103/physrevb.107.l020403 (2023).

[31] Y. Li, P.-P. Zhang, L.-Z. Hu, Y. Xu, and X.-M. Kong, Ground-state and thermal entanglements in non-hermitian XY system with real and imaginary magnetic fields, Quantum Inf Process **22**, 277 (2023).

[32] D. Toulouse, Geometric phase and phase diagram for a non-hermitian quantum XY model, Comm. Phys. **2**, 115 (1977).

[33] J. Mydosh, Spin glasses— recent experiments and systems, Journal of Magnetism and Magnetic Materials **7**, 237 (1978).

[34] K. Binder and A. P. Young, Spin glasses: Experimental facts, theoretical concepts, and open questions, Rev. Mod. Phys. **58**, 801 (1986).

[35] M. Mezard, G. Parisi, and M. Virasoro, *Spin Glass Theory and Beyond* (World Scientific, 1986) https://www.worldscientific.com/doi/pdf/10.1142/0271.

[36] P. Charbonneau, E. Marinari, M. Mézard, G. Parisi, F. Ricci-Tersenghi, G. Sicuro, and F. Zamponi, *Spin Glass Theory and Far Beyond* (World Scientific, 2023) https://www.worldscientific.com/doi/pdf/10.1142/13341.

[37] P. Jordan and E. Wigner, Über das paulische Äquivalenzverbot, Zeitschrift für Physik **47**, 631 (1928).

[38] T. J. Osborne and A. Stottmeister, Conformal field theory from lattice fermions, Communications in Mathematical Physics **398**, 219 (2023).

[39] M. A. Metlitski, The XY model in one dimension, (2004).

[40] V. T. S. R. Derzhko, O. and R. J., Square-lattice $s = 12$ XY model and the jordan–wigner fermions: the ground-state and thermodynamic properties, Physica A: Statistical Mechanics and its Applications **320**, 407 (2003).

[41] C. J. I. Verstraete, F. and J. I. Latorre, Quantum circuits for strongly correlated quantum systems, Phys. Rev. A **79**, 032316 (2009).

[42] T. S. Elliott, L. and M. Daniel, Two soluble models of an antiferromagnetic chain, Annals of Physics **16**, 407 (1961).

[43] T. Krokhmalskii, T. Verkholyak, O. Baran, V. Ohanyan, and O. Derzhko, Spin-$\frac{1}{2}$ xx chain in a transverse field with regularly alternating g factors: Static and dynamic properties, Phys. Rev. B **102**, 144403 (2020).

[44] P. Calabrese, M. Mintchev, and E. Vicari, The entanglement entropy of one-dimensional systems in continuous and homogeneous space, Journal of Statistical Mechanics: Theory and Experiment **2011**, P09028 (2011).

[45] M. Collura, M. Kormos, and P. Calabrese, Stationary entanglement entropies following an interaction quench in $1D$ bose gas, Journal of Statistical Mechanics: Theory and Experiment **2014**, P01009 (2014).

[46] S.-A. Cheong and C. L. Henley, Many-body density matrices for free fermions, Phys. Rev. B **69**, 075111 (2004).

[47] I. Peschel, Calculation of reduced density matrices from correlation functions, Journal of Physics A: Mathematical and General **36**, L205–L208 (2003).

[48] P. Calabrese, Entanglement and thermodynamics in non-equilibrium isolated quantum systems, Physica A: Statistical Mechanics and its Applications **504**, 31 (2018), lecture Notes of the 14th International Summer School on Fundamental Problems in Statistical Physics.

[49] P. Calabrese and J. Cardy, Entanglement entropy and quantum field theory, Journal of Statistical Mechanics: Theory and Experiment **2004**, P06002 (2004).

[50] L.-M. Chen, Y. Zhou, S. A. Chen, and P. Ye, Quantum entanglement of non-hermitian quasicrystals, Physical Review B **105**, 10.1103/physrevb.105.l121115 (2022).

[51] A. K. Pati, Entanglement in non-hermitian quantum theory, Pramana **73**, 485–498 (2009).